Indian Journal of Engineering & Materials Sciences
Vol. 25, June 2018, pp. 233-242

Study of hardness and wear behavior of surface modified AA 7075 with tungsten carbide using GTA as a heat source

J Abhinavaram, A Shanmugasundaram*, R Prashanth, S Jagadeesh, Sanjivi Arul & R Sellamuthu

Department of Mechanical Engineering, Amrita School of Engineering, Amrita Vishwa Vidyapeetham, Coimbatore 641 112, India

Received 20 January 2017; accepted 10 July 2017

The aim of this work is to evaluate the role of tungsten carbide (WC) in increasing the hardness and improving the wear resistance of AA 7075 alloy. WC is reinforced into the surface of AA 7075 by using gas tungsten arc (GTA) as a heat source. Some of the GTA process parameters are maintained as constant, viz, contact-to-work distance and electrode tip angle, whereas the heat source current and the work speed are varied. With reference to the proper fusion of base metal, optimum GTA heat source parameter is finalized based on a number of trials. It is found that the hardness is reduced after the application of heat. To improve the properties, the alloy is subjected to heat treatment which included solution treatment, water quenching, and artificial aging. The hardness and wear behavior of the WC reinforced surface composite resulted in a positive trend. A comprehensive study on the microstructure of AA 7075 at different stages of the work is done using optical microscopy (OM), scanning electron microscopy (SEM), EDX analysis and X-ray diffraction (XRD).

Keywords: AA 7075, Dry sliding wear, GTA, Hardness, Heat treatment, Surface reinforcement, Tungsten carbide

In recent years, the demand for light weight and high strength materials like aluminium alloys have increased steadily. These aluminium alloys are of immense use in automobile, aircraft and aerospace applications due to their excellent strength-to-weight ratio and their resistance properties in adverse environments[1]. Aluminium alloys are used in the automobile sector for the production of cylinder blocks, cylinder heads and pistons for internal combustion engines. However, the application of aluminium alloy is limited due to their limited hardness and poor wear behavior[2].

The elemental composition of the bulk of Zn-Al alloys[3] and Al-Zn-Cu alloys[4] have been altered by using stir casting technique. Wear rates of Al-6Zn-4Mg alloys tested at different conditions were also investigated[5]. The influence of GTAW process on the hardness and microstructure by shallow cryogenic treatment was also studied[6].The effect of fly ash and Al_2O_3 reinforced A 356 alloy matrix hybrid composites was investigated[7]. In-situ reinforcements of ceramic particles and its effect on AA 7075 hardness and wear resistance were also studied. In-situ reinforcement of TiB_2 was reported to have enhanced wear behavior[2]. These works involved changing the entire properties of the bulk. Although there is an increase in hardness and wear behavior of these bulk modification methods, as the reinforced particles get distributed non-homogeneously in the matrix, uniform properties may not be obtained. Since hardness and wear behavior of an alloy are surface phenomena, surface modification methods can be employed in the place of bulk modification techniques like casting.

Surface modifications can be done by thermal applications, mechanical stirring, chemical and physical vapor deposition, laser cladding, plasma spraying, electron beam facing, friction stir processing, plating or depositing a protective layer onto the surface of AA 7075. It was already reported there is an improvement in the mechanical properties of AA 7075 plate when the surface is reinforced with SiC nanoparticles by friction stir processing[8]. Plasma-assisted nitriding of aluminium alloys was done to improve the wear properties[9]. Laser cladding of WC ceramic particles on steel was done to solve many tribological problems related to steel[10]. However, the cost of laser cladding applications is high. The wear behavior of steel was improved by applying an austenitic nitrous coating on the surface by electron beam facing[11]. Surface reinforcement of SiC on AA

*Corresponding author
(E-mail: a_shanmugasundaram@cb.amrita.edu)

7075 –T651 using friction stir processing resulted in better wear properties[12]. Not much work was done in reinforcing the surface of AA 7075 alloy with hard ceramic particles using gas tungsten arc (GTA) as a heat source. GTA is a versatile process where the process variables can be controlled easily with the fabrication of clean and spatter free welds of appreciable weld quality. AA 7075 in the T6 temper condition has a heterogeneous microstructure, consisting of an Al matrix, secondary phase particles and grain boundary regions. Alloying elements are added to 7xxx alloys mainly for precipitation hardening. Zinc and magnesium offer the highest potential for strengthening through age-hardening and chromium aids in increasing the stress corrosion cracking (SCC) resistance[13].

Tungsten carbide (WC), belongs to Group VI interstitial carbides. It is an extremely hard refractory ceramic material, similar to titanium carbide. WC finds its applications in cutting and drilling tools, drawing and extrusion die, sealing rings, etc. Coatings of WC are deposited in thermal and plasma CVD to improve the surface properties[14].

In this study, an attempt is made to modify the surface of AA 7075 alloy by reinforcing tungsten carbide (WC) particulates onto the surface by using GTA as a heat source. The main objective of this study is to improve the hardness and wear resistance of the material. Material characterization is done using an optical microscope (OM) and scanning electron microscope (SEM). Also, EDX analysis and X-ray diffraction (XRD) are done to confirm the presence of elements.

Materials and Methods

Lincoln Electric V205T GTAW equipment is used for applying heat over the surface of the AA 7075. A PLC based stepper motor driven manipulator is used to control the speed of the work specimen, which is kept over the work-table. The position of the torch is held stationary in the vertically down position. Inert gas argon is used as a shielding gas at 7 L/min flow rate. Thoriated tungsten electrode of diameter 2.4 mm is used during welding to have the better arc stability. Direct current electrode negative (DCEN) mode is used for applying the heat over the surface of AA 7075. A schematic representation of the experimental setup is shown in Fig. 1. The raw material AA 7075 aluminium alloy having the size of 25 mm width × 12 mm thickness cut into required number of pieces. Trial runs performed on the base metal by varying current (100 A to 200 A), work speed (1 to 10 mm/s) and the electrode to work distance (1 to 5 mm). Thoriated tungsten electrode frequently grounded to maintain an angle of 60° at the tip. It was found that if the heat source current was below 150 A, the work speed is above 10 mm/s and the electrode to work distance was greater than 2mm then the lack of fusion was observed. If the current is above 150 A, work speed was below 2 mm/s and electrode to work distance were below 2 mm burn through were observed. The final heat source parameters reported in Table 1. The procured WC powder is sieved using an auto sieve shaker for various grit sizes of 75, 90, 106 and 150 μm. WC particles with an average grit size of 106 μm were used. The WC ceramic particle bonded with the base AA 7075 surface by using hydrolyzed polyvinyl alcohol (PVA). Otherwise, the particle will fly over to other areas due to the flow of argon gas during the process. The specimens are heated in the furnace to remove the moisture. Using optimized GTA parameter the WC particles are deposited onto the surface of the substrate. To enhance the mechanical properties, the samples are heat-treated.

AA 7075 is a heat treatable alloy, the heat applied samples and the surface reinforced composites were subjected to heat treatment to regain their properties

Table 1 — Optimized GTA parameters

GTA process parameters	Value
Heat source current	150 A
Voltage	20 V
Distance between electrode and workpiece	2 mm
Work speed	6 mm/s
Electrode tip angle	60°

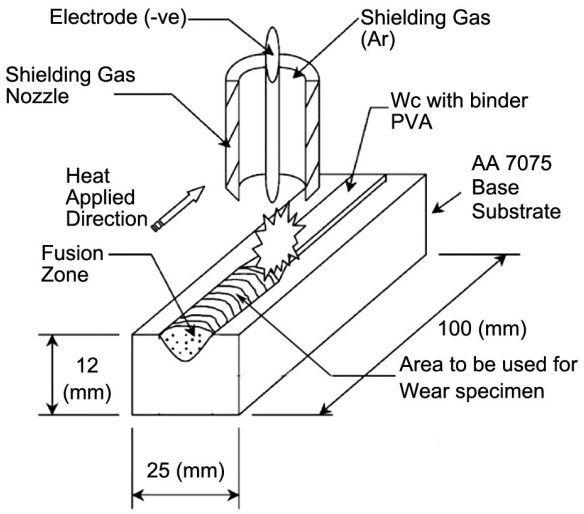

Fig. 1 — Schematic diagram of GTA process setup

which would have been degraded upon the application of heat. Heat treatment includes solution treatment at 480°C for 2 h; followed by water quenching for 15 minutes; andfinally, artificial ageing at 120°C for 4, 8, 12, 16, 20, 22, 24, 26 and 28 h to find out the optimum artificial aging time with respect to maximum hardness.

Dry sliding wear tests for the composites were conducted using the pin-on-disc machine (Ducom TR -20). It is attached with Ducom Wear & Friction Monitor (TR - 2OLE - PHM 200). The parameters taken for dry sliding wear test are loads of 10 N - 30 N in steps of 10 N, the velocity of 1 m/s – 2 m/s in steps of 0.5 m/s and with the constant sliding distance of 1000 m. Tests were conducted according to ASTM 99-95a standard. The pin (Ø8 mm × 25 mm) is held stationary against the counterface of a 100 mm diameter rotating disc made of EN-31 steel having a hardness of 60 HRC. The load was applied to the sample by a cantilever mechanism. After each test, the disc is cleaned to remove debris. Before and after each test the weight of specimens is measured by an electronic weighing balance. Wear rate is determined as the ratio of weight loss divided by the product of the density and sliding distance.

The specimens were polished by standard metallographic methods and were etched with Keller's reagent (150 mL H_2O, 3mL HNO_3 and 6 mL HF). The etched samples were observed using a Carl Zeiss metallurgical microscope. SEM analyses were done to have a better understanding of the alloy and to reveal the presence of WC particles in the aluminium matrix. EDX and XRD analyses were also carried out to confirm the presence of WC particles in AA 7075.

Results and Discussion

The elements present in the base material confirmed by the laser spectroscopic analysis. Table 2 shows the chemical composition of the base material using optical emission spectrometer (METAVISION - 1008 I). Hardness measurements are carried on the base metal, fusion zone of the heat applied specimens and WC reinforced AA 7075 using Mitutoyo (MVK-H11) Vickers microhardness testing equipment. The microhardness is measured with 100 g-force load for 15 s. Minimum 10 points are used to get the average microhardness. The average microhardness of the base metal is 167 HV.

This high hardness of the alloy, when compared to other aluminium alloys, is attributed to the presence of precipitates throughout the alloy matrix. Precipitates are found to nucleate and grow during aging as a result of supersaturation of alloying elements after solution treatment. The most notable precipitates are the η and ή phases of $MgZn_2$ and the associated solute-rich clusters, known as GP zones. These precipitates are responsible for providing the high strength to the alloy, are typically several nanometers in size, and are present along the grain boundaries. Other precipitates identified include Mg_2Al_3, Al_2Cu, and $Al_{32}Zn_{49}$[15,16].

Table 2 — Elemental composition of as received AA 7075

Element	Composition (wt%)
Al	89.940
Zn	5.180
Mg	2.275
Cu	1.690
Fe	0.466
Cr	0.204
Si	0.060
Pb	0.059
Mn	0.056
Ti	0.052
Zr	0.013
Ca	0.002
Sr	0.002

The heat input to the bead-on-plate welding for the different trials are calculated using the Eq. (1)[17].

$$q/v = \frac{EI\eta}{V} \quad \ldots (1)$$

Where q/v is the heat input (J/mm), E is the voltage (V), I is the current (A), V is the working specimen speed (mm/s), and η is the efficiency of GTA = 0.74[18].

The variation of heat input with reference to the work speed and heat source current is calculated using Eq. (1) and are as follows: With respect to the heat source current of 150 A and work speed of 2, 4 and 6 mm/s the heat inputs were 1110, 555 and 370 J/mm, correspondingly. Whereas for the heat source current 175 A and torch speed of 2, 4 and 6 mm/s the heat inputs were 1295, 648 and 432 J/mm correspondingly.

The optical micrograph of the AA 7075 base metal is portrayed in Fig. 2a.

The image shows elongated grains and dark patches distributed over the aluminium matrix. These dark patches are the constituent particles. The sizes of these particles range from 10 to 20 µm. These constituent particles are composed of Al_2CuMg, Al_7Cu_2Fe, Al_3Fe and $(Al,Cu)_6(Fe,Cu)$. These particles

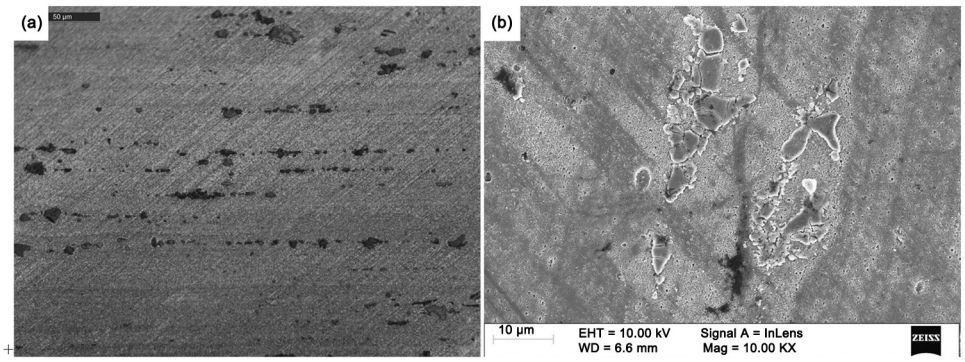

Fig. 2 — (a) The optical microstructure of AA 7075 base metal at 500X and (b) FE-SEM image of AA 7075 base metal at 10,000X

are formed during solidification and will often break up and align during working and forming of the metal. They are not affected by further heat treatment[15,16,19]. Investigations are already indicated that $MgZn_2$ precipitates are the reason for the high hardness of the AA 7075 alloy. Apart from this, GP zones and ή precipitates contribute mainly to the high strength of AA 7075 - T6 matrix, of which, the contribution of ή precipitates to the strength was reported to be higher[20].

The FE - SEM microstructure of the surface of AA 7075 at a magnification of 10,000X shown in Fig. 2b.

Lighter patches of the constituent particles and cavities are observed. Cavities occur where particles have been either removed or dissolved during polishing of the specimens. To identify the phases which dominate these constituent particles, EDX analysis is performed.

The EDX line scans in Figs 3(a) and 3(b), indicate the presence of zinc, magnesium, copper and iron in the larger particles, while the cavities reveal the presence of silicon. The EDX spectrum analyses also indicate that the distribution of zinc, copper and magnesium is relatively uniform in the alloy matrix. It has been reported that the large constituent particles consist of Al_7Cu_2Fe, Al_2Cu (θ-phase) and Al_3Fe (β-phase), while smaller particles containing magnesium and silicon consist of Mg_2Si (β-phase). Magnesium and zinc precipitate along the grain boundaries as $MgZn_2$ (η-phase)[15,16,19].

The microhardness of the fusion zone of the heat applied samples are measured and their hardness profiles are depicted in Figs 4(a) and 4(b). With reference to the hardness measurement, the following inference can be concluded: (i) The reduction of hardness on the fusion zone from the base metal with the heat source current of 150 A was 32%, 31% and

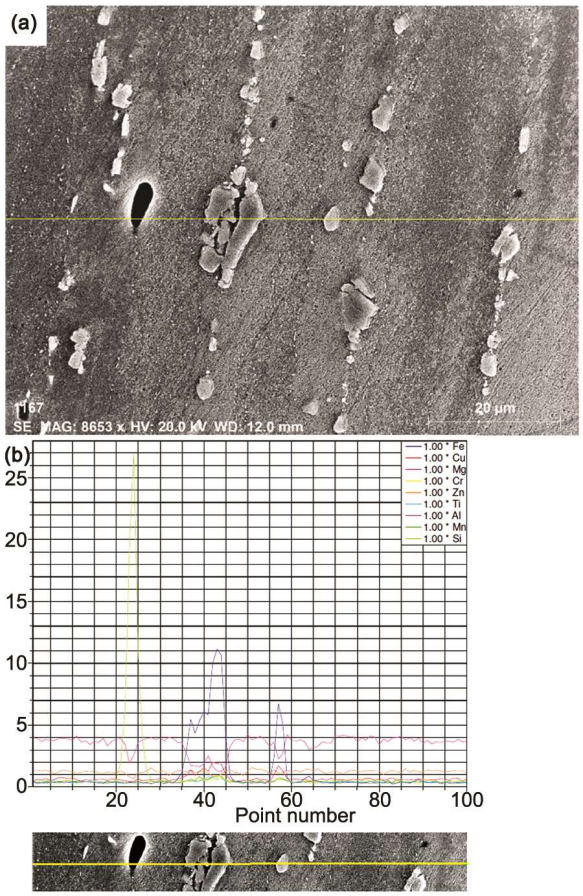

Fig. 3 — (a) FE-SEM microstructure during line EDX of base metal; and (b) enlarged line EDX scan of AA 7075 base metal

26% with respect to the work speed of 2, 4 and 6 mm/s correspondingly; (ii) Whereas the reduction of hardness on the fusion zone from the base metal with the heat source current of 175 A was 39%, 36% and 31% with respect to the work speed of 2, 4 and 6 mm/s correspondingly.

It is inferred from the above tests that the maximum hardness reduction takes place at the fusion zone. This behavior can be attributed to the

dissolution of precipitates and increase in aluminium grain size which occur during the application of heat to the samples[21]. The over aging and dissolution of ή precipitates and coarsening of grains in the aluminium matrix due to the application of large amounts of heat is the prime reason for the reduction in hardness of the fusion zone[20]. However, the presence of some fine equiaxed grains and the resolution of the dissolved precipitates partially remedy the loss of hardness. The reason behind the hardness variation across the fusion zone is found to be temperature difference due to the difference in solidification rate at different positions of the heat applied zone. The extreme left and right of the fusion zone are closer to the base metal and thereby the heat is dissipated easily to the substrate. Whereas at the center of the fusion zone, heat input was constant, however, the heat dissipation was much lesser compared to other places of the fusion zone. This caused the center of the fusion zone to have lower hardness when compared to other places of the fusion zone.

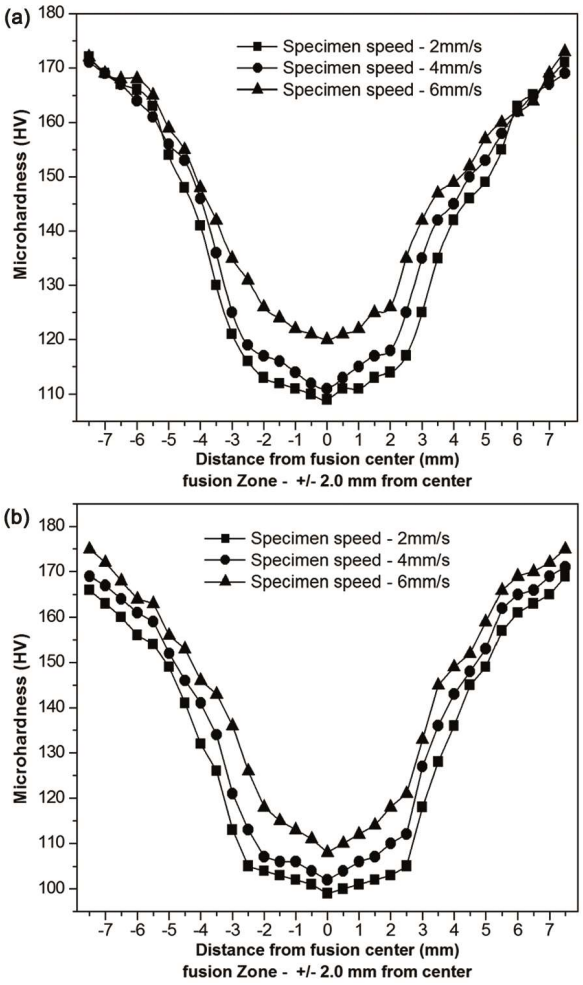

Fig. 4 — Microhardness of heat applied sample with the heat source current of (a) 150 A and (b) 175 A

From the six trials, the least average hardness in the fusion zone is observed to be 102 HV with the heat source current of 175A and work speed of 2 mm/s. The reduction from the base metal hardness of 167 HV is 65 HV (39%). The maximum hardness is observed with the heat source current of 150 A and work speed of 6 mm/s. The average hardness is 124 HV and the reduction in hardness of the base metal is only 43 HV (26%). According to the heat input calculations, when the heat input increases the hardness reduces correspondingly.

The optical microstructure of the fusion zones of both the specimens are observed at 500X and are shown in Figs 5(a) and 5(b).These images reveal that the grains of the specimens processed using the heat source current of 175 A and 2 mm/s of work speed are much coarser than the grains of the other specimens processed using the heat source current of 150 A and 6 mm/s of work speed. The specimen with a heat source current of 150 A and works peed of 6 mm/s experiences lower heat input and this enables the heat to be easily dissipated to the base metal and the effect of heat is reduced. Hence, the solidification will

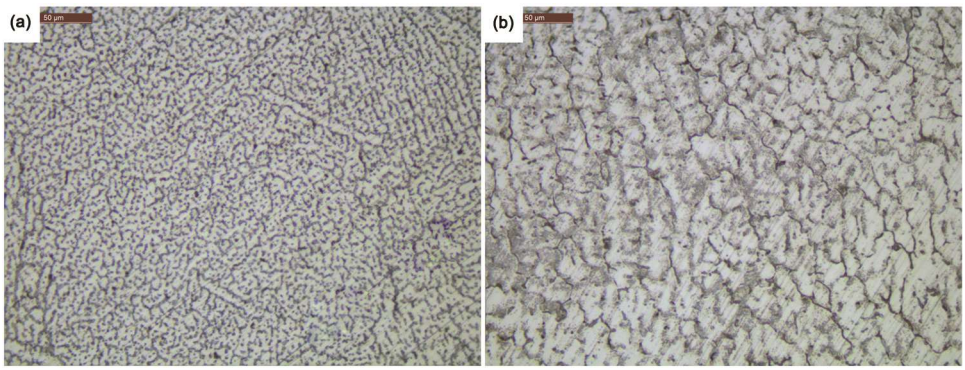

Fig. 5 — Microstructure of fusion zone taken at 500 X of heat applied samples with the heat source current of (a) 150 A and (b) 175 A

happen at a faster rate, which leads to the formation of finer grains. Whereas, the specimen with a heat source current of 175 A and works peed of 2 mm/s has a higher heat input, and the rate of solidification is slower as the heat dissipation to the base metal is much lesser. This is the reason for the formation of coarser grains in this sample.

The finer grains in the 150 A and 6 mm/s specimen is the reason for its higher hardness at the fusion zone when compared to the other specimen. This micrographic study further elucidates the higher hardness of the former. This is according to the Hall–Petch equation that hardness increases as grain size decreases[22]. In addition, the small particles of the intermetallic compounds formed help in improving hardness according to Orowan hardening mechanism[23].

Based on the microstructure analyses and hardness profiles of the fusion zones, further WC reinforcement will be carried out by using the heat source current of 150 A and the work speed of 6 mm/s, as our ultimate aim is to increase the hardness of AA 7075 by reinforcing ceramic particles.

Figure 6(a) shows the FE–SEM microstructure of the heat applied specimen revealing the fusion zone, heat affected zone (HAZ) and base metal observed at 2,000X. The image portrays the difference in constituent particle sizes of the fusionzone, heat affected zone and base metal. The constituent particles of the fusion zone are much coarser than those of the heat affected zone. This is because of the higher temperature and slower solidification rate in the fusion zone when compared to the heat affected zone (HAZ). Like-wise, the constituent particles of the base metal are finer than the particles of the HAZ. This is because the base metal has the lowest temperature compared to HAZ and fusion zone.

The WC particles are deposited with the heat source current of 150 A and work speed of 6mm/s. The hardness of the reinforced samples are measured along the fusion zone, heat affected zone and the base metal. The average hardness at the fusion zone was measured to be 147 HV. This is 23 HV higher than the heat applied sample hardness of 124 HV. The increase in hardness is because of the reinforcement of WC particles into the aluminium matrix. These particles result in the formation of high-angle boundaries in the aluminium matrix. These high-angle boundaries prevent the dislocations from moving on the application of load and thereby increase the hardness and strength of the fusion zone. This is according to Orawan mechanism[24].

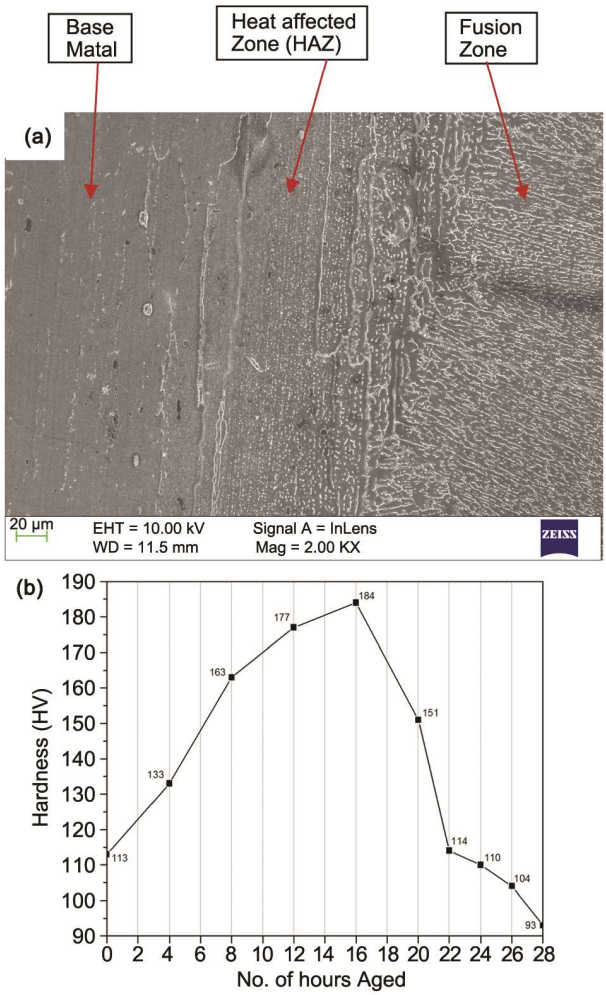

Fig. 6 — (a) FE –SEM microstructure of heat applied sample at 2000 X and (b) average hardness of the WC reinforced zone for different artificially aged time periods

AA 7075 is a heat treatable wrought aluminium alloy, the hardness of the reinforced zone can be further increased by carrying out heat Treatment[20]. The hardness of the solution treated and quenched samples were measured to be 113 HV. This is far less than the reinforced hardness of 147 HV. This is because of the dissolution of precipitates in the solid solution as a result of keeping the specimen for the specified period. In order to improve the hardness, the solution treated samples were artificially aged at 120°C. The average hardness of the fusion zone for a time period ranging from 4-28 h is shown in Fig. 6(b). It is inferred from Fig. 6(b) that the highest hardness of 184 HV was attained after 16 h of aging. The hardness decreases after 16 h due to over ageing. The reason for this high hardness is the reinforcement of WC particles in the fusion zone. These particles prevent the dislocations from moving and thereby

increase the hardness. In addition to this, the presence of uniform and continuous grain structure and strengthening precipitates, formed at 16 h of artificial ageing at the grain boundaries are the reasons for the increased hardness[20].

The artificially aged, WC reinforced samples were thoroughly studied using FE–SEM, EDX and XRD techniques. The FE-SEM microstructure of the reinforced AA 7075 is shown Fig. 7(a) reveal that the WC particles are embedded onto the AA 7075 base matrix. The density difference between the aluminium matrix and ceramic particle significantly contributes to the distribution of ceramic particles during solidification. The ceramic particles begin to sink when the density of the ceramic particle is higher than the matrix material. Suspension of ceramic particles for a long time in the molten aluminium is desired to obtain homogeneous distribution. The ceramic particles can remain suspended in the molten matrix for a longer duration, provided the density difference between the substrate and ceramic particle is more than 2 g/cm[325]. As the density difference between AA 7075 alloy substrate and WC particles is nearly 13 g/cm^3, the WC particles remain suspended in the fusion zone for a longer duration. In addition to this, free movement of the ceramic particles is hindered by the wetting action of the molten aluminium matrix[2]. These factors result in the better distribution of WC particles in the fusion zone.

It is evident from the FE – SEM microstructure further taken at higher magnification reveals the interface between the WC particles and the matrix is clean and WC particles are well bonded in the aluminium matrix. Thermodynamic stability of WC particles in the molten matrix is the reason for the clear interface. Undesirable compounds are formed at the interface when a ceramic particle is thermodynamically unstable in the fusion zone[26,27]. In our case, there is no formation of such undesirable compounds as is evident from the XRD analysis.

Point EDX analysis is performed on the surface composite to confirm the presence of the elements of tungsten and carbon, which constitute WC. The elemental composition of the EDX result shown in Fig. 7(b) reveals the presence of W and C. XRD analysis of the WC reinforced surface composite reveals the patterns of compounds and is shown in Fig. 8. The diffraction peaks of the tungsten carbide are clearly visible. The peaks of the main precipitates of the alloy matrix, viz., magnesium zinc and

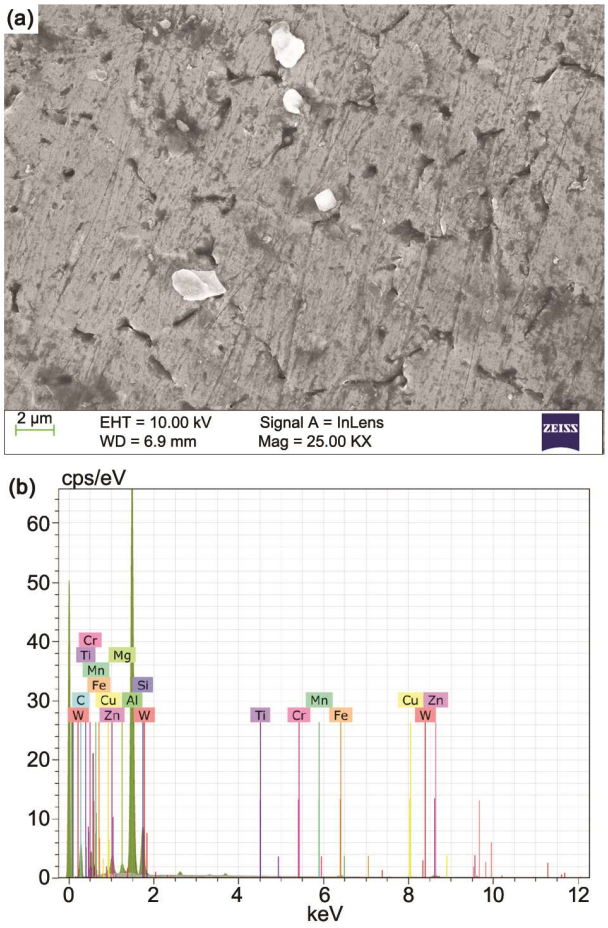

Fig. 7 — (a) FE-SEM microstructure of WC reinforced AA 7075 at 10000 X and (b) point EDX scan of the surface composite

magnesium silicide are also present. The pattern lists along with the reference code are given as: Tungsten carbide (WC) presence is confirmed with the reference code of 01-079-0743; tungsten was present with the reference code of 01-088-2339; magnesium zinc ($MgZn_2$) was present on the diffused zone with the reference code of 01-071-9628; and magnesium silicide (Mg_2Si) was also present with the reference code of 01-077-9648.

This proves that the WC particles are present in the aluminium matrix. It is also inferred from Fig. 8 that there is no formation of any other compound as a result of reinforcing WC in the aluminium matrix. This indicates that WC particles are thermodynamically stable and the interface between aluminium alloy and WC particles tends to be free.

Wear behavior of the base metal, heat applied sample and WC reinforced specimen are investigated. The effect of load on the wear rate of the specimen for constant sliding velocity is plotted in Fig. 9(a). Similarly, the effect of sliding velocity on the wear

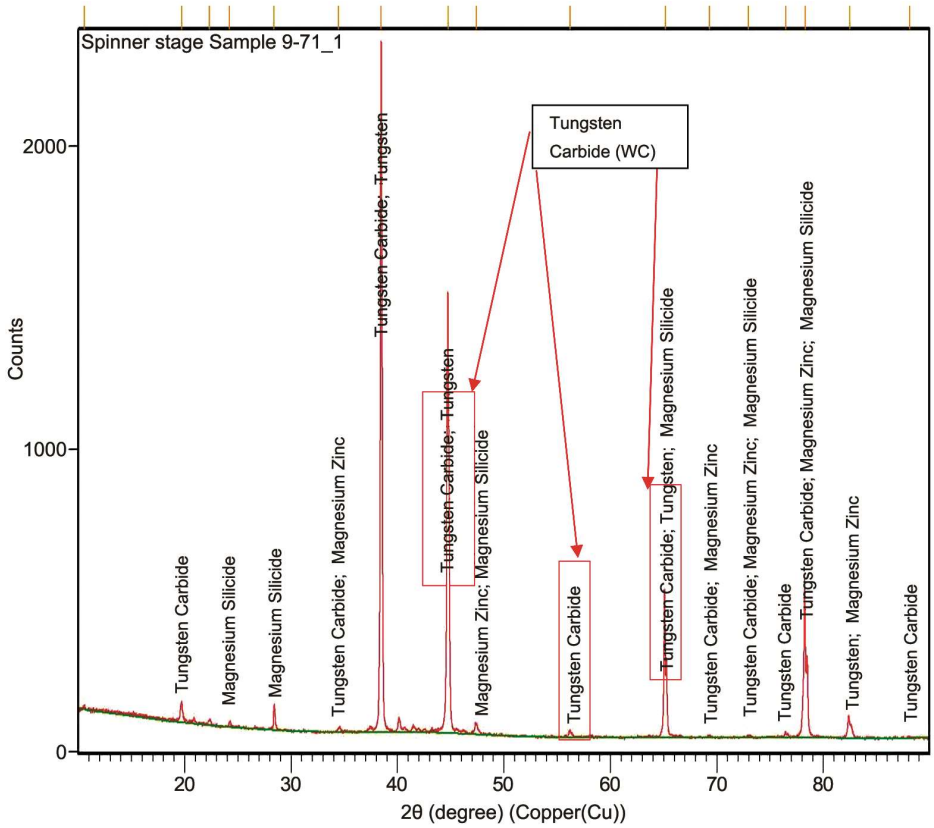

Fig. 8 — XRD Analysis of the surface composite

rate of the specimen for the constant load is plotted in Fig. 9(b). From the Fig. 9(a) it can be inferred that in the case of base metal, the sliding wear is initiated when the relatively moving counter surfaces make asperity-to-asperity contact. The counterface steel disc is relatively harder than the composite specimen. The initial stage of wear consists of fragmentation of the asperities and removal of material due to the cutting of hard asperities into the softer pin surface. When the load increases, the temperature increases due to friction and this leads to softening of the aluminium matrix. This results in enhanced penetration of the hard asperities of the counter surface into the pin, which causes more metal removal. The effect is well pronounced when the load is further increased leading to higher wear rate.

The wear rate of the heat-applied samples is lesser than that of the base metal. This is because of the dissolution of precipitates, which strengthen the aluminium matrix upon the application of heat. It can also be inferred that the wear behavior of AA 7075 has been enhanced by the reinforcement of WC particles on the surface. This is because of the interactions between dislocations and WC particles, which resist the propagation of cracks during sliding wear. Strain fields are created around WC particles due to the thermal mismatch between the aluminium alloy and WC particle during solidification. These strain fields offer resistance to the propagation of the cracks and subsequent material removal[3]. The homogeneous distribution of WC particles provides Orawan strengthening. The clear interface and good bonding delay the detachment of particles from the aluminium matrix. The presence of WC particles resists the cutting action of counter-face asperities and reduces wear rate. Therefore, wear resistance of the surface composites is enhanced by the WC particulate content. In all the three cases, viz., base metal, heat applied and WC reinforced specimen, wear rate increases as the load increases. Previous investigations reveal the same result[5].

Wear rate is maximum at a load of 30 N at a sliding velocity of 1 m/s and is 0.00427 mm^3/m, 0.00605 mm^3/m and 0.00355 mm^3/m of the base metal, heat applied sample and WC reinforced specimen respectively. Wear rate is minimum for a load of 10 N at a sliding velocity of 2 m/s and are 0.00071 mm^3/m, 0.00107 mm^3/m and 0.00035 mm^3/m of the base

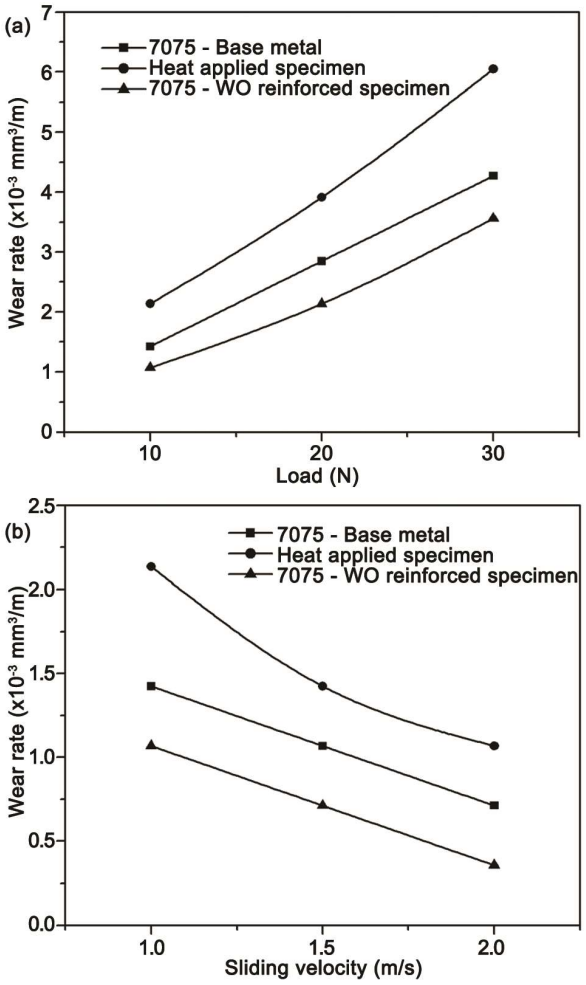

Fig. 9 — (a) Load vs wear rate with the constant sliding velocity of 1 m/s and (b) sliding velocity vs wear rate for the constant load of 10 N

metal, heat applied sample and WC reinforced specimen respectively.

From Fig. 9(b) it can be inferred that wear rate decreases as sliding velocity increases. Higher sliding velocities imply higher frictional force between the pin surface and the counter face, and thus an increase in temperature. At higher temperatures, the pin surface becomes soft and forms an oxide layer[28,29]. This oxide layer facilitates smoother sliding of the pin over the counter surface and hence results in lower wear rate. The variation of wear rates in the case of 10 N load and 2 m/s sliding velocity for base metal, heat applied sample and WC reinforced specimen are depicted in Fig. 10. The reduction in wear rate of the WC reinforced composite w.r.t. the base metal is 50%.

The density of WC is 15.8 cm^3. WC density is almost 6 times greater than the density of the base

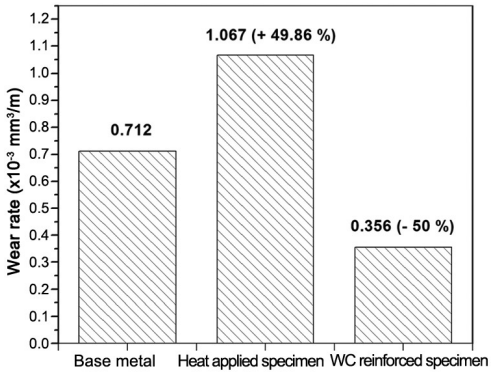

Fig. 10 — Variation of wear rate for the load of 10 N and a sliding velocity of 2 m/s

structure AA 7075 (2.80 cm^3). In addition, the melting point of WC is 2870ºC whereas the melting point of base substrate AA 7075 is 635ºC only. During the GTA process, the top surface of the base substrate does not reach the temperature required for melting WC. During the reinforcement of WC ceramic particle on to top surface of base substrate, the denser WC ceramic particle embedded on to the molten aluminium alloy forming AA 7075-WC surface composite. This is the reason during wear test; the wear resistance of the AA 7075-WC surface composite is well above that of the base metal.

Conclusions

In the present work, AA 7075 – WC surface composites are fabricated by using gas tungsten arc (GTA) as a heat source. The effectiveness of WC particles to improve the hardness and wear properties are investigated. The following conclusions are drawn:

(i) The hardness of the fusion zone decreased upon the application of heat on the base metal. This is because of the dissolution of precipitates and coarsening of constituent particles.

(ii) A minimum hardness reduction of 26% was observed in the case of a heat source current of 150 A and with a work speed of 6 mm/s. The average hardness of the fusion zone was 124 HV.

(iii) The WC particles were bonded well to the aluminium matrix with clean interfaces.

(iv) Heat treatment further increased the hardness to significant levels and enhanced the wear resistance.

(v) The maximum hardness of 184 HV is observed in the fusion zone after 16 h of artificial ageing. The hardness increase is about 10% from the base hardness of 167 HV.

(vi) The reinforcement of WC particles on to the surface enhanced the wear resistance of the surface composite. The minimum wear rate of 0.000356 mm^3/m is obtained at a load of 10 N and at a sliding velocity of 2 m/s and this is 50% less than the base metal wear rate of 0.000712 mm^3/m.

(vii) XRD analysis of the surface composite revealed that the WC particles are thermodynamically stable in the aluminium matrix, as no inter-metallic compounds are formed.

References

1 Ravikumar S, Seshagiri Rao V & Atish Ranjan, 2nd *Int Conf on Trends in Industrial and Mechanical Engineering,*(*ICTIME'2013*), Hong Kong, Sept 17-18, 2013.

2 Michael Rajan H B, Ramabalan S, Dinaharan I & Vijay S J, *Arch Civil Mech Eng,*14 (2014) 72-79.

3 Kasthuri Raj S R, Ilangovan S, Sanjivi Arul & Shanmugasundaram A, *Int J Appl Eng Ch,* 10(2) (2015) 2723-2731.

4 Suresh K K, Ilangovan S, Sanjivi Arul & Shanmugasundaram A, *Int J Appl Eng Ch,*10(4) (2015) 9325-9333.

5 Ramasundaram A, Ilangovan S, Sanjivi Arul & Shanmugasundaram A, *Int J Appl Eng Ch,* 10(6) (2015) 15417-15428.

6 Devanathan R, Sanjivi Arul, Ilangovan S & Shanmugasundaram A, *Int J Appl Eng Ch,* 10(8) (2015) 21091-21099.

7 Kulkarni S G, Menghani J V & Achchhe Lal, *Indian J Eng Mater Sci*, 23 (2016) 27-36.

8 Mohsen Bahrami, Mohammad Kazem Besharati Givi, Kamran Dehghani & Nader Parvin, *Mater Des,* 53 (2014) 519–527.

9 Quast M, Stock H R & Mayr P, *Met Sci Heat Treat*, 46 (2004) 7-8.

10 Smurov I, Doubenskaia M, Grigoriev S N, Kotoban D V & Podrabinnik P A, *J Frict Wear,* 35(6) (2014) 470-476.

11 Tagiltseva D N, Narkevich N A, Shulepov I A & Moiseenko D D, *J Frict Wear,* 35(2) (2014) 104-110.

12 Sert A and Celik O N, *Indian J Eng Mater S*, 21 (2014) 35-43.

13 Ian Polmear, *Light Alloys from Traditional Alloys to Nanocrystals, 4th ed,* (Elsevier's Science and Technology), 2006.

14 Huge O Pierson, *Handbook of Refractory Carbides and Nitrides- Properties, Characteristics, Processing and Applications*,1st ed, (Noyes Publications), 1996.

15 Polmear I J, *Light Alloys: Metallurgy of the Light Metals - Metallurgy & Materials Science*, 3rd ed, (Wiley and Sons, New York), 1996.

16 Nie J, Muddle B & Polmear I, *Mater Sci Forum,* 217-222 (1996) 1257-1262.

17 Poorhaydari K, Patchett B M & Ivey D G, *Weld Res*, (2005) 149-155.

18 Arul S & Sellamuthu R, *Int J Comput Mater Sci Surface Eng*, 4(3) (2011).

19 Maloney S, Polmear I & Ringer S, *Mater Sci Forum,* 331-337 (2000) 1055-1060.

20 Vijaya Kumar P, Madhusudhan Reddy G & Srinivasa Rao K, *Def Technol*, (2015) 1-8.

21 Ceschini L, Boromei I, Minak G, Morri A & Tarterini F, *Compos Sci Technol*, 67 (2007) 605-615.

22 Rajakumar S, Muralidharan C & Balasubramanian V, *Mater Des*, 32 (2011) 535-549.

23 Wang X H & Wang K S, *Mater Sci Eng,* 431 (2006) 114-117.

24 Sudhakar I, Madhusudhan Reddy G & Srinivasa Rao K, *Def Technol,* (2015) 1-7.

25 Han Y, Liu X & Bian X, *Compos Part A-Appl S*, 33(3) (2002) 439-444.

26 Ashok Kumar B & Murugan N, *Mater Des*, 40(1) (2012) 52-58.

27 DavidsonA M & Regener D, *Compos Sci Technol*, 60(6) (2000) 865-869.

28 Kumar S, Subramanya Sarma V & Murty B S, *Wear*, 268(11-12) (2010) 1266-1274.

29 Ilangovan S, Shanmugasundaram A & Sanjivi Arul, *J Surf Sci Technol*, 32 (3-4) (2016) 93-98.